

IEM-FT-153/97
hep-ph/9703412

CONSTRAINTS ON THE HIGGS BOSON PROPERTIES FROM THE EFFECTIVE POTENTIAL ^a

M. QUIROS

*Instituto de Estructura de la Materia (CSIC),
Serrano 123, 28006-Madrid, SPAIN*

We review the constraints on Higgs boson properties from effective potential methods. In the Standard Model, the requirement of stability (or metastability) of the standard electroweak minimum puts an upper bound on the scale of new physics as a function of the Higgs mass. This upper bound is below the Planck scale if the Higgs weights $\lesssim 130$ GeV. In supersymmetric extensions of the Standard Model the former methods are useful to compute the Higgs mass spectrum, and couplings, after resumming higher loop effects. In particular, if the Higgs mass weights $\gtrsim 130$ GeV, the minimal supersymmetric extension of the Standard Model will be ruled out, while its non-minimal supersymmetric extension containing singlets is only marginally allowed.

1 Introduction

The effective potential ¹⁻⁷ (the effective action at zero external momentum) V_{eff} is a very useful tool to compute the vacuum of a quantum field theory, and thus to determine its mass spectrum. The effective potential admits a loop expansion as:

$$V_{\text{eff}} = \sum_{n=0}^{\infty} V_n \quad (1)$$

and its calculation involves (at $n \geq 1$) a mass parameter μ upon which it explicitly depends. For instance in mass-independent renormalizations schemes, which are those usually employed, as $\overline{\text{MS}}$ ⁸, or $\overline{\text{DR}}$ ⁹, the one-loop effective potential can be written in the 't Hooft-Landau gauge as

$$V_1 = \frac{1}{64\pi^2} \text{Str } m^4 \left[\log \frac{m^2}{\mu^2} - C \right], \quad (2)$$

where the supertrace operator counts positively (negatively) the number of degrees of freedom for the different bosonic (fermionic) fields, C is a (constant) diagonal matrix which depends on the renormalization scheme, and μ

^aTo appear in *Perspectives on Higgs Physics II*, Ed. G.L. Kane, World Scientific, Singapore.

is the renormalization group scale on which all dimensionless and dimensional couplings of the theory depend.

Being μ an unphysical scale, the effective potential should not depend on the choice of it. This property can be achieved if a change in the scale μ can be compensated by appropriate changes in the couplings and field rescalings. Mathematically it can be formulated by a renormalization group equation (RGE) satisfied by the effective potential, which admits as solution:

$$V_{\text{eff}} \equiv V_{\text{eff}}(\mu(t), \lambda_i(t); \phi_a(t)) \quad (3)$$

where $\lambda_i(t)$ are all the (running) parameters of the theory, the scale $\mu(t)$ is related to the running parameter t by

$$\mu(t) = \mu e^t \quad (4)$$

and the running (Higgs) fields are ($a = 1, \dots, N$)

$$\phi_a(t) = \xi_a(t) \phi_a \equiv e^{- \int_0^t \gamma_a(t') dt'} \phi_a \quad (5)$$

where ϕ_a are the classical fields on which the generating functional of 1PI Green functions depend, and $\gamma_a(t)$ are the corresponding anomalous dimensions. We are assuming here that the fields ϕ_a have different quantum numbers and so they are not mixed by radiative corrections. Of course this situation is not the most general one, but it corresponds to the cases that will be studied in this paper: the Standard Model (SM), with a single Higgs doublet, the Minimal Supersymmetric Standard Model (MSSM), which contains two Higgs doublets with opposite hypercharges, and its extension with one singlet superfield.

Now the complete effective potential (3) and its n^{th} derivative matrix, defined by

$$V_{\text{eff}}^{a_1 \dots a_n} = \xi_{a_1}(t) \dots \xi_{a_n}(t) \frac{\partial^n}{\partial \phi_{a_1}(t) \dots \partial \phi_{a_n}(t)} V_{\text{eff}} \quad (6)$$

satisfies the scale-independence condition

$$\frac{d V_{\text{eff}}^{a_1 \dots a_n}}{dt} = 0 \quad (7)$$

By defining the running masses by

$$\overline{m}_{ab}^2(t) = \frac{\partial^2}{\partial \phi_a(t) \partial \phi_b(t)} V_{\text{eff}} \Big|_{\langle \phi(t) \rangle}, \quad (8)$$

and using the scale independence of the effective potential (7), we obtain the scale variation:

$$\frac{d \overline{m}_{ab}^2(t)}{dt} = [\gamma_a(t) + \gamma_b(t)] \overline{m}_{ab}^2(t) \quad (9)$$

Of course the running masses are not physical quantities since they depend on the renormalization scale as in (9), and also on the gauge and renormalization scheme, as the effective potential does. However, one can compute, from the running masses the physical (pole) masses as follows. The inverse of the renormalized propagator with momentum p can be written ^b on general grounds as

$$\Gamma_{ab}(p^2) = p^2 \delta_{ab} - [m_{ab}^2 + \Pi_{ab}(p^2)] \quad (10)$$

where m_{ab}^2 are the renormalized masses and $\Pi_{ab}(p^2)$ are the $\overline{\text{MS}}$, or $\overline{\text{DR}}$ -renormalized self energies, obtained by subtracting from the corresponding unrenormalized quantities (regulated via dimensional regularization) the divergent terms proportional to $1/\epsilon - \gamma_E + \log 4\pi$, where the space-time dimensionality is written as $D = 4 - 2\epsilon$ and γ_E is the Euler constant.

The relation between the running mass \overline{m}_{ab} and the inverse propagator,

$$\Gamma_{ab}(0) = -\overline{m}_{ab}^2(t) \quad (11)$$

allows to write the relation between the renormalized and the running masses, as

$$\overline{m}_{ab}^2 = m_{ab}^2 + \Pi_{ab}(0) \quad (12)$$

and hence the inverse propagator is usually written as

$$\Gamma_{ab}(p^2) = p^2 \delta_{ab} - [\overline{m}_{ab}^2 + \Delta\Pi_{ab}(p^2)] \quad (13)$$

$$\Delta\Pi_{ab}(p^2) \equiv \Pi_{ab}(p^2) - \Pi_{ab}(0) \quad (14)$$

The physical masses are then defined as the poles of the diagonalized inverse propagator (13), or the solution to the equation,

$$\det [p^2 \delta_{ab} - (m_{ab}^2 + \Pi_{ab}(p^2))] = 0 \quad (15)$$

or, equivalently,

$$\det [p^2 \delta_{ab} - (\overline{m}_{ab}^2 + \Delta\Pi_{ab}(p^2))] = 0 \quad (16)$$

In a diagrammatic calculation the physical masses are obtained as solutions of Eq. (15). Then, after computing the matrix $m_{ab} + \Pi_{ab}(p^2)$ and finding its eigenvalues $\mu_A^2(p^2)$, ($A = 1, \dots, N$), the physical (pole) masses M_A are the solutions of the equations

$$M_A^2 = \mu_A^2(M_A^2) \quad (17)$$

^bSince we are mainly interested in masses (not widths) we understand implicitly that we are considering the real parts of the inverse propagators and of the self-energies.

which is obviously the solution to Eq. (15). Of course, Eqs. (15) and (16) are completely equivalent and both have the same solution. Obviously diagrammatic methods, solving Eq. (15), and effective potential methods, solving Eq. (16), yield the same result, at they should. However effective potential methods have the advantage that \overline{m}_{ab}^2 already contains the dominant part of the one-loop corrections and Eq. (16) can be most easily solved approximately. The way of proceeding is by diagonalization of the matrix of running masses \overline{m}_{ab}^2 with eigenvalues \overline{m}_A^2 , ϕ_A being the new mass eigenstate fields. The physical masses M_A are then given by,

$$M_A^2 = \overline{m}_A^2 + \Delta\Pi_{AA}(M_A^2) \quad (18)$$

where the self-energies in (18) are computed in the mass eigenstate basis ϕ_A .

Let us notice that, unlike the running masses, \overline{m}_A , the pole masses M_A do not depend on the renormalization scale, this fact being guaranteed by the invariance of the effective action with respect to the scale, and hence by the renormalizability of the theory. In practical calculations this invariance can be considered as a cross-check of the result. For the case of the SM this has been explicitly shown¹⁰.

The contents of this article are as follows. In Section 2 the effective potential methods will be applied to the Standard Model. In particular lower stability (and metastability) bounds and upper perturbativity bounds will be obtained for the pole Higgs mass. Section 3 will be devoted to the MSSM, where the radiatively corrected spectrum of Higgs masses and couplings will be deduced from effective potential methods. Section 4 will contain results on upper bounds on the lightest Higgs boson mass in extensions of the MSSM: in particular extensions containing Higgs singlets, where the properties of gauge coupling constant unification observed at LEP are not spoiled. Section 5 tries to answer the question on, what if a light Higgs (with a mass below ~ 130 GeV) is discovered at LEP2 or FNAL? Finally Section 6 contains some general conclusions. The self-energies, $\Delta\Pi_{ab}$ relating running and physical masses for the cases of the Standard Model and MSSM are listed in Appendices A and B, respectively.

2 The Standard Model

In the SM the Higgs boson is an $SU(2)_L$ doublet with hypercharge 1/2 given by:

$$H = \begin{pmatrix} \chi^+ \\ \phi + i\chi^0 \\ \sqrt{2} \end{pmatrix} \quad (19)$$

where ϕ is the physical Higgs, that must acquire a vacuum expectation value (VEV) $v = (\sqrt{2}G_F)^{-1/2}$. The fields $\chi^{\pm 0}$ are Goldstone bosons, which become massless in the vacuum of the theory. Therefore, the effective potential for the SM depends on a single background field ϕ .

The renormalization group improved effective potential of the SM, V , can be written in the 't Hooft-Landau gauge and the \overline{MS} scheme as⁵

$$V[\mu(t), \lambda_i(t); \phi(t)] \equiv V_0 + V_1 + \dots, \quad (20)$$

where $\lambda_i \equiv (g, g', \lambda, h_t, m^2)$ runs over all dimensionless and dimensionful couplings and V_0, V_1 are the tree level potential and the one-loop correction, respectively, namely

$$V_0 = -\frac{1}{2}m^2(t)\phi^2(t) + \frac{1}{8}\lambda(t)\phi^4(t), \quad (21)$$

$$V_1 = \sum_{i=1}^5 \frac{n_i}{64\pi^2} m_i^4(\phi) \left[\log \frac{m_i^2(\phi)}{\mu^2(t)} - c_i \right] + \Omega(t), \quad (22)$$

$\Omega(t)$ being the one-loop contribution to the cosmological constant⁵, and

$$m_i^2(\phi) = \kappa_i \phi^2(t) - \kappa'_i, \quad (23)$$

with non-zero coefficients $n_W = 6, \kappa_W = g^2(t)/4, c_W = 5/6; n_Z = 3, \kappa_Z = [g^2(t) + g'^2(t)]/4, c_Z = 5/6; n_t = -12, \kappa_t = h_t^2(t)/2, c_t = 3/2; n_\phi = 1, \kappa_\phi = 3\lambda(t)/2, \kappa'_\phi = m^2(t), c_\phi = 3/2; n_\chi = 3, \kappa_\chi = \lambda(t)/2, \kappa'_\chi = m^2(t), c_\chi = 3/2$.

It has been shown⁶ that the L-loop effective potential improved by (L+1)-loop RGE resums all Lth-to-leading logarithm contributions. Consequently, we will consider all the β - and γ -functions of the previous parameters to two-loop order, so that our calculation will be valid up to next-to-leading logarithm approximation.

As has been pointed out⁵, working with $\partial V/\partial\phi$ (and higher derivatives) rather than with V itself allows to ignore the cosmological constant term Ω . In fact, the structure of the potential can be well established once we have determined the values of ϕ , say ϕ_{ext} , at which V has extremals (maxima or minima), thus we only need to evaluate $\partial V/\partial\phi$ and $\partial^2 V/\partial\phi^2$. From Eq. (20), the value of ϕ_{ext} is given by

$$\left. \frac{\partial V}{\partial\phi(t)} \right|_{\phi(t)=\phi_{\text{ext}}(t)} = 0 \Rightarrow \phi_{\text{ext}}^2(t) = \frac{2m^2 + \sum_i \frac{n_i \kappa_i \kappa'_i}{8\pi^2} \left[\log \frac{m_i^2(\phi)}{\mu^2(t)} - c_i + \frac{1}{2} \right]}{\lambda + \sum_i \frac{n_i \kappa_i^2}{8\pi^2} \left[\log \frac{m_i^2(\phi)}{\mu^2(t)} - c_i + \frac{1}{2} \right]}. \quad (24)$$

The second derivative is given by

$$\frac{\partial^2 V}{\partial \phi^2(t)} \bigg|_{\phi(t)=\phi_{\text{ext}}(t)} = 2m^2 + \sum_i \frac{n_i \kappa_i \kappa'_i}{8\pi^2} \left[\log \frac{m_i^2(\phi)}{\mu^2(t)} - c_i + \frac{1}{2} \right] + \phi^2(t) \sum_i \frac{n_i \kappa_i^2}{8\pi^2}, \quad (25)$$

where we have used (24). Eq. (25) can be written in a more suggestive form as

$$\begin{aligned} \frac{\partial^2 V}{\partial \phi^2(t)} \bigg|_{\phi(t)=\phi_{\text{ext}}(t)} &= 2m^2 + \frac{1}{2}(\beta_\lambda - 4\gamma\lambda)\phi^2(t) \\ &+ \frac{1}{2}(\beta_{m^2} - 2\gamma m^2) \left[\sum_{i, \kappa'_i \neq 0} \log \frac{m_i^2(\phi)}{\mu^2(t)} - 2 \right], \end{aligned} \quad (26)$$

where β_λ , β_{m^2} and γ are one-loop β - and γ -functions.

We would like to stress the fact that even though the whole effective potential is scale-invariant, the one-loop approximation is *not*. Therefore, one needs a criterion to choose the appropriate renormalization scale in the previous equations. A sensible criterion¹⁰ is to choose the scale, say $\mu^* = \mu(t^*)$, where the effective potential is more scale-independent. μ^* turns out to be a certain average of the $m_i(\phi)$ masses. Actually, it was shown¹⁰ that any choice of μ^* around the optimal value produces the same results for physical quantities up to tiny differences.

The running mass m_H^2 , defined as the second derivative of the renormalized effective potential (see Eqs. (8) and (9)), is given by

$$m_H^2 = \frac{\partial^2 V_{\text{eff}}}{\partial \phi^2} = -\Gamma_R(p^2 = 0) = m_R^2 + \Pi_R(p^2 = 0) . \quad (27)$$

where m_R is the renormalized mass, while the physical (pole) mass satisfies the relation

$$M_H^2 = m_R^2 + \Pi_R(p^2 = M_H^2) . \quad (28)$$

Comparing (28) and (27) we have

$$M_H^2 = m_H^2 + \Delta\Pi, \quad (29)$$

where we have defined (we drop the subscript R from Π_R)

$$\Delta\Pi \equiv \Pi(p^2 = M_H^2) - \Pi(p^2 = 0). \quad (30)$$

The complete expression for the quantity $\Delta\Pi$ is given in appendix A.

2.1 Stability bounds

The solution to (24) describes the standard electroweak (EW) minimum, but might also describe other maxima and non-standard minima. The preliminary question one should now ask is: When the standard EW minimum becomes metastable, due to the appearance of a deep non-standard minimum? This question was addressed in past years¹¹ taking into account leading-log (LL) and part of next-to-leading-log (NTLL) corrections. More recently, calculations have incorporated all NTLL corrections^{12,13} resummed to all-loop by the renormalization group equations, and considered pole masses for the top-quark and the Higgs-boson. From the requirement of a stable (not metastable) standard EW minimum we obtain a lower bound on the Higgs mass, as a function of the top mass, labelled by the values of the SM cutoff (stability bounds). Our result¹³ is lower than previous estimates.

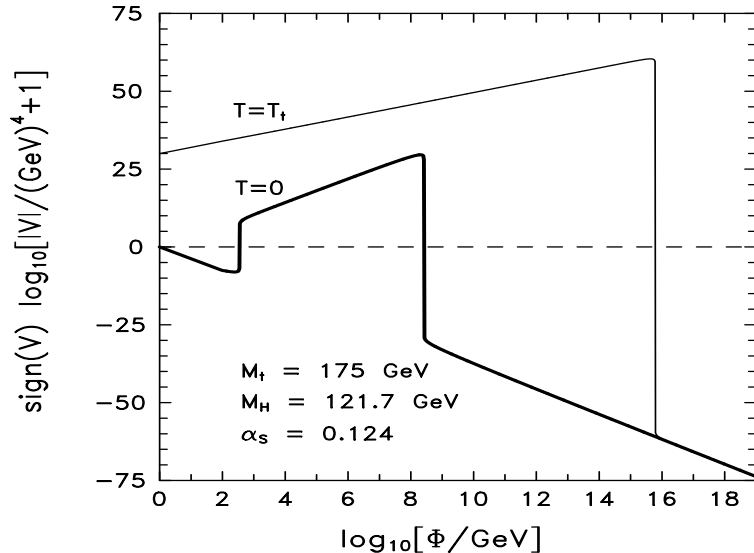


Figure 1: Plot of the effective potential for $M_t = 175$ GeV, $M_H = 121.7$ GeV at $T = 0$ (thick solid line) and $T = T_t = 2.5 \times 10^{15}$ GeV (thin solid line).

The problem to attack is easily stated as follows. The condition (24) is obviously satisfied at the EW minimum where $\langle\phi\rangle = v \sim 246$ GeV, $\lambda \sim (m_H/v)^2 > 1/16$, $m^2 \sim m_H^2/2$ and $V''(\langle\phi\rangle) > 0$ (a minimum). However, it can also be satisfied for values of the field $\phi \gg v$ and, since $m = \mathcal{O}(100)$ GeV, for

those values

$$\lambda \sim \left(\frac{m}{\phi} \right)^2 \ll 1.$$

Therefore, for the non-standard extremals we have

$$\begin{aligned} \beta_\lambda < 0 &\implies V'' < 0 \text{ maximum} \\ \beta_\lambda > 0 &\implies V'' > 0 \text{ minimum.} \end{aligned} \quad (31)$$

The one-loop effective potential of the SM improved by two-loop RGE has been shown to be highly scale independent¹⁰ and, therefore, very reliable for the present study. In Fig. 1 we show (thick solid line) the shape of the effective potential for ^c $M_t = 175$ GeV and $M_H = 121.7$ GeV. We see the appearance of the non-standard maximum, ϕ_M , while the global non-standard minimum has been cutoff at $M_{P\ell}$. We can see from Fig. 1 the steep descent from the non-standard maximum. Hence, even if the non-standard minimum is beyond the SM cutoff, the standard minimum becomes metastable and might be destabilized. So for fixed values of M_H and M_t the condition for the standard minimum not to become metastable is

$$\phi_M \gtrsim \Lambda \quad (32)$$

Equation (32) makes the stability condition Λ -dependent. In fact we have plotted in Fig. 2 the stability condition on M_H versus M_t for $\Lambda = 10^{19}$ GeV and 10 TeV. The stability region corresponds to the region above the dashed curves. Accurate fits of the bounds on M_H are,

$$M_H[\text{GeV}] > 52 + 0.64(M_t[\text{GeV}] - 175) - 0.50 \frac{\alpha_s(M_Z) - 0.12}{0.006} \quad (33)$$

for $\Lambda = 1$ TeV, and

$$M_H[\text{GeV}] > 133 + 1.92(M_t[\text{GeV}] - 175) - 4.28 \frac{\alpha_s(M_Z) - 0.12}{0.006} \quad (34)$$

for $\Lambda = 10^{19}$ GeV.

We want to conclude this section with a few comments about the errors affecting our analysis¹³. Errors come from: a) The evaluation of the top-quark pole mass M_t , where we have neglected two-loop QCD and one-loop

^c M_t stands for the physical (pole) top-quark mass, as opposite to the top-quark running mass defined in (23).

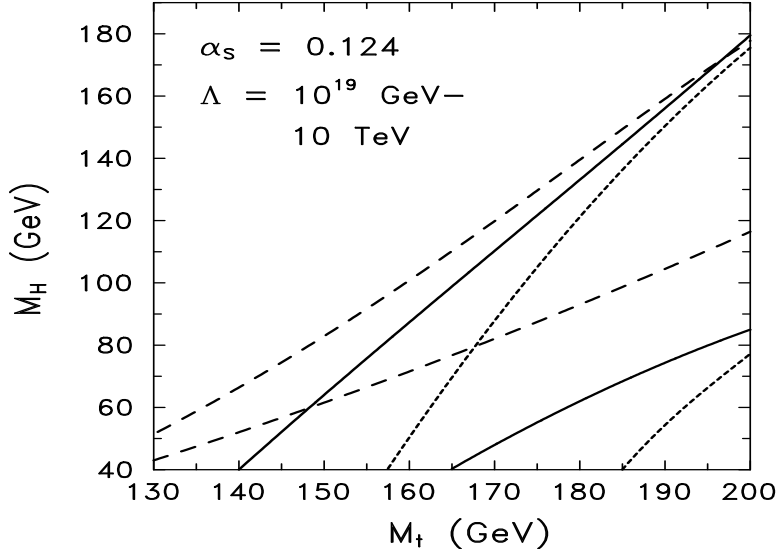


Figure 2: Lower bounds on M_H as a function of M_t , for $\Lambda = 10^{19}$ GeV (upper set) and $\Lambda = 10$ TeV (lower set). The dashed curves correspond to the stability bounds and the solid (dotted) ones to the metastability bounds at finite (zero) temperature.

electroweak corrections; b) Higher (two)-loop corrections which have been neglected in the effective potential; c) The fact that bounds are computed in a particular (Landau) gauge. The gauge dependence of the result can be translated into an error ^d in the lower bound. All together we have estimated the total uncertainty as

$$\Delta M_H \lesssim 5 \text{ GeV} \quad (35)$$

^dThe gauge dependence of the bound has recently been stressed¹⁵ in a toy model, with a U(1) gauge symmetry and fermion fields which mimic the effect of the top quark in the Standard Model, whose effective potential in a class of gauges parametrized by a real parameter ξ ($\xi = 0$ in Landau gauge) has been worked out. The effective potential, as well as the β and γ -functions, depends on the RGE invariant combination ξg^2 . These authors have pointed out that for extremely large values of the parameter ξg^2 the effect of the one-loop correction to the effective potential on the Higgs mass bound blows up. This is just a reflection of the failure of perturbation theory, and higher loop corrections should affect dramatically the results of Ref. ¹⁵ for these values of ξg^2 . However, for moderate values of the parameter ξg^2 for which two-loop/one-loop corrections are small (and perturbation theory valid), the uncertainty in the bound mass from the gauge dependence of the result is small and expected to be, for the case of the Standard Model, inside the range of (35).

2.2 Metastability bounds

In the last subsection we have seen that in the region of Fig. 2 below the dashed line the standard EW minimum is metastable. However we should not draw physical consequences from this fact since we still do not know at which minimum does the Higgs field sit. Thus, the real physical constraint we have to impose is avoiding the Higgs field sitting at its non-standard minimum. In fact the Higgs field can be sitting at its zero temperature non-standard minimum if:

1. The Higgs field was driven from the origin to the non-standard minimum at finite temperature by thermal fluctuations in a non-standard EW phase transition at high temperature. This minimum evolves naturally to the non-standard minimum at zero temperature. In this case the standard EW phase transition, at $T \sim 10^2$ GeV, will not take place.
2. The Higgs field was driven from the origin to the standard minimum at $T \sim 10^2$ GeV, but decays, at zero temperature, to the non-standard minimum by a quantum fluctuation.

In Fig. 1 we have depicted the effective potential at $T = 2.5 \times 10^{15}$ GeV (thin solid line) which is the corresponding transition temperature. Our finite temperature potential¹⁴ incorporates plasma effects¹⁶ by one-loop resummation of Debye masses¹⁷. The tunnelling probability per unit time per unit volume was computed long ago for thermal¹⁸ and quantum¹⁹ fluctuations. At finite temperature it is given by $\Gamma/\nu \sim T^4 \exp(-S_3/T)$, where S_3 is the euclidean action evaluated at the bounce solution ϕ_B . The semiclassical picture is that unstable bubbles are nucleated behind the barrier at $\phi_B(0)$ with a probability given by Γ/ν . Whether or not they fill the Universe depends on the relation between the probability rate and the expansion rate of the Universe. By normalizing the former with respect to the latter we obtain a normalized probability P , and the condition for decay corresponds to $P \sim 1$. Of course our results are trustable, and the decay actually happens, only if $\phi_B(0) < \Lambda$, so that the similar condition to (32) is

$$\Lambda < \phi_B(0) \quad (36)$$

The condition of no-decay (metastability condition) has been plotted in Fig. 2 (solid lines) for $\Lambda = 10^{19}$ GeV and 10 TeV. The region between the dashed and the solid line corresponds to a situation where the non-standard minimum exists but there is no decay to it at finite temperature. In the region below the solid lines the Higgs field is sitting already at the non-standard minimum at $T \sim 10^2$ GeV, and the standard EW phase transition does not happen. A

fit for $\Lambda = 10^{19}$ GeV is

$$M_H[\text{GeV}] > 125 + 2.28(M_t[\text{GeV}] - 175) - 4.89 \frac{\alpha_s(M_Z) - 0.12}{0.006} \quad (37)$$

As for the gauge dependence, we expect it to affect very little the previous results. The total potential at finite temperature is entirely dominated, for $\phi < \phi_B(0)$, by the thermal correction (see Fig. 1). But the one-loop thermal correction coming from gauge boson and the top-quark propagation, as well as the improvement due to thermal masses, is gauge independent²⁰, while all the gauge dependence is encoded in the contribution from Higgs and Goldstone bosons, which would affect very little the result.

We also have evaluated the tunnelling probability at zero temperature from the standard EW minimum to the non-standard one. The result of the calculation should translate, as in the previous case, in lower bounds on the Higgs mass for different values of Λ . The corresponding bounds are shown in Fig. 2 in dotted lines. Since the dotted lines lie always below the solid ones, the possibility of quantum tunnelling at zero temperature does not impose any extra constraint.

As a consequence of all improvements in the calculation, our bounds are lower than previous estimates²¹. To fix ideas, for $M_t = 175$ GeV, the bound reduces by ~ 10 GeV for $\Lambda = 10^4$ GeV, and ~ 30 GeV for $\Lambda = 10^{19}$ GeV.

2.3 Perturbativity bounds

Up to here we have described lower bounds on the Higgs mass based on stability arguments. Another kind of bounds, which have been used in the literature, are upper bounds based on the requirement of perturbativity of the SM up to the high scale (the scale of new physics) Λ .

Since the quartic coupling grows with the scale ϵ , it will blow up to infinity at a given scale: the scale where λ has a Landau pole. The position of the Landau pole Λ is, by definition, the maximum scale up to which the SM is perturbatively valid. In this way assuming the SM remains valid up to a given scale Λ amounts to requiring an upper bound on the Higgs mass from the perturbativity condition²²

$$\frac{\lambda(\Lambda)}{4\pi} \leq 1 \quad (38)$$

This upper bound depends on the scale Λ and very mildly on the top-quark mass M_t through its influence on the renormalization group equations of λ .

²⁰In fact the value of the renormalization scale where the quartic coupling starts growing depends on the value of the top-quark mass.

We have plotted in Fig. 3 this upper bound for different values of the high scale Λ , along with the corresponding stability bounds.

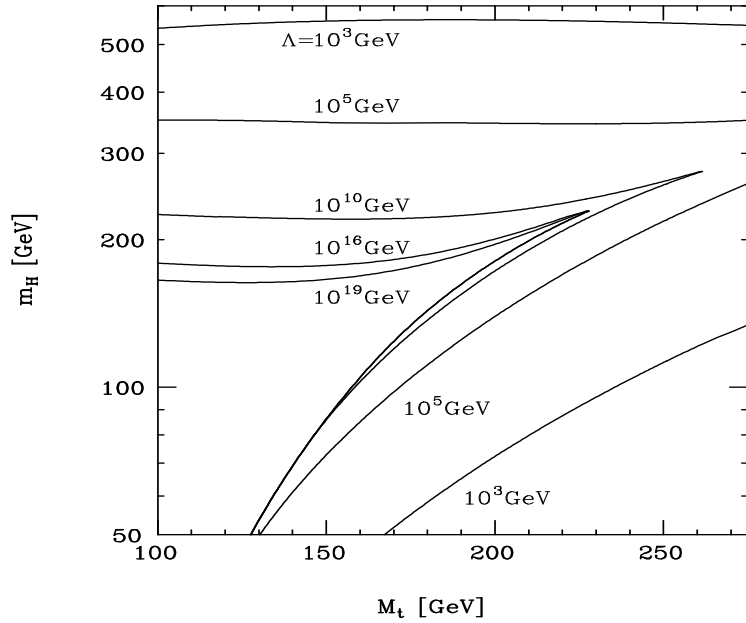


Figure 3: Perturbativity and stability bounds on the SM Higgs boson. Λ denotes the energy scale where the particles become strongly interacting.

3 The Minimal Supersymmetric Standard Model

The Minimal Supersymmetric Standard Model (MSSM)²³ is the best motivated extension of the SM where some of their theoretical problems (e.g. the hierarchy problem inherent with the fact that the SM cannot be considered as a fundamental theory for energies beyond the Planck scale) find (at least) a technical solution. The Higgs sector of the MSSM²⁴ requires two Higgs

doublets, with opposite hypercharges, as

$$\begin{aligned} H_1 &= \begin{pmatrix} H_1^0 \\ H_1^- \end{pmatrix}_{-1/2} \\ H_2 &= \begin{pmatrix} H_2^+ \\ H_2^0 \end{pmatrix}_{1/2} \end{aligned} \quad (39)$$

The reason for this duplicity is twofold. On the one hand it is necessary to cancel the triangular anomalies generated by the higgsinos. On the other hand it is required by the structure of the supersymmetric theory to give masses to all fermions.

The most general gauge invariant scalar potential is given, for a general two-Higgs doublet model, by:

$$\begin{aligned} V = & m_1^2 |H_1|^2 + m_2^2 |H_2|^2 + (m_3^2 H_1 H_2 + h.c.) + \frac{1}{2} \lambda_1 (H_1^\dagger H_1)^2 \\ & + \frac{1}{2} \lambda_2 (H_2^\dagger H_2)^2 + \lambda_3 (H_1^\dagger H_1)(H_2^\dagger H_2) + \lambda_4 (H_1 H_2)(H_1^\dagger H_2^\dagger) \\ & + \left\{ \frac{1}{2} \lambda_5 (H_1 H_2)^2 + [\lambda_6 (H_1^\dagger H_1) + \lambda_7 (H_1^\dagger H_2^\dagger)] (H_1 H_2) + h.c. \right\} \end{aligned} \quad (40)$$

However, supersymmetry provides the following tree-level relations between the previous couplings:

$$\begin{aligned} \lambda_1 &= \lambda_2 = \frac{1}{4} (g^2 + g'^2) \\ \lambda_3 &= \frac{1}{4} (g^2 - g'^2), \quad \lambda_4 = -\frac{1}{4} g^2 \\ \lambda_5 &= \lambda_6 = \lambda_7 = 0 \end{aligned} \quad (41)$$

Replacing (41) into (40) one obtains the tree-level potential of the MSSM, as:

$$\begin{aligned} V_{\text{MSSM}} = & m_1^2 H_1^\dagger H_1 + m_2^2 H_2^\dagger H_2 + m_3^2 (H_1 H_2 + h.c.) \\ & + \frac{1}{8} g^2 (H_2^\dagger \vec{\sigma} H_2 + H_1^\dagger \vec{\sigma} H_1)^2 + \frac{1}{8} g'^2 (H_2^\dagger H_2 - H_1^\dagger H_1)^2 \end{aligned} \quad (42)$$

This potential, along with the gauge and Yukawa couplings in the superpotential,

$$W = h_u Q \cdot H_2 U^c + h_d Q \cdot H_1 D^c + h_\ell L \cdot H_1 E^c + \mu H_1 \cdot H_2 \quad (43)$$

determine all couplings and masses (at the tree-level) of the Higgs sector in the MSSM.

3.1 Tree-level mass relations

After gauge symmetry breaking,

$$\begin{aligned} v_1 &= \langle \text{Re } H_1^0 \rangle \\ v_2 &= \langle \text{Re } H_2^0 \rangle \end{aligned} \quad (44)$$

the Higgs spectrum contains one neutral CP-odd Higgs A (with mass m_A , that will be taken as a free parameter)

$$A = \cos \beta \text{Im} H_2^0 + \sin \beta \text{Im} H_1^0 \quad (45)$$

and one neutral Goldstone χ^0

$$\chi^0 = -\sin \beta \text{Im} H_2^0 + \cos \beta \text{Im} H_1^0 \quad (46)$$

with $\tan \beta = v_2/v_1$. It also contains one complex charged Higgs H^\pm ,

$$H^+ = \cos \beta H_2^+ + \sin \beta (H_1^-)^* \quad (47)$$

with a (tree-level) mass

$$m_{H^\pm}^2 = m_A^2 + (\lambda_5 - \lambda_4)v^2, \quad (48)$$

and one charged Goldstone χ^\pm ,

$$\chi^+ = -\sin \beta H_2^+ + \cos \beta (H_1^-)^*. \quad (49)$$

Finally the Higgs spectrum contains two CP-even neutral Higgs bosons H, \mathcal{H} (the light and the heavy mass eigenstates) which are linear combinations of $\text{Re } H_1^0$ and $\text{Re } H_2^0$, with a mixing angle α given by

$$\sin 2\alpha = \frac{2M_{12}^2}{\sqrt{(\text{Tr} M^2)^2 - 4 \det M^2}} \quad (50)$$

$$\cos 2\alpha = \frac{M_{11}^2 - M_{22}^2}{\sqrt{(\text{Tr} M^2)^2 - 4 \det M^2}} \quad (51)$$

and masses

$$m_{H(\mathcal{H})}^2 = \frac{\text{Tr} M^2 \mp \sqrt{(\text{Tr} M^2)^2 - 4 \det M^2}}{2} \quad (52)$$

where

$$Tr M^2 = M_{11}^2 + M_{22}^2 ; \quad \det M^2 = M_{11}^2 M_{22}^2 - (M_{12}^2)^2 , \quad (53)$$

with

$$\begin{aligned} M_{12}^2 &= 2v^2[\sin \beta \cos \beta (\lambda_3 + \lambda_4) + \lambda_6 \cos^2 \beta + \lambda_7 \sin^2 \beta] - m_A^2 \sin \beta \cos \beta \\ M_{11}^2 &= 2v^2[\lambda_1 \cos^2 \beta + 2\lambda_6 \cos \beta \sin \beta + \lambda_5 \sin^2 \beta] + m_A^2 \sin^2 \beta \\ M_{22}^2 &= 2v^2[\lambda_2 \sin^2 \beta + 2\lambda_7 \cos \beta \sin \beta + \lambda_5 \cos^2 \beta] + m_A^2 \cos^2 \beta . \end{aligned} \quad (54)$$

where ($v^2 = v_1^2 + v_2^2$) the couplings λ_i are taken at their tree level values (41), yielding

$$m_{H^\pm}^2 = M_W^2 + m_A^2 \quad (55)$$

and

$$m_{H,\mathcal{H}}^2 = \frac{1}{2} \left[m_A^2 + M_Z^2 \mp \sqrt{(m_A^2 + M_Z^2)^2 - 4m_A^2 M_Z^2 \cos^2 2\beta} \right] \quad (56)$$

3.2 The Higgs tree level couplings

All couplings in the Higgs sector are functions of the gauge (G_F, g, g') and Yukawa couplings, as in the SM, and of the previously defined mixing angles β, α . Some relevant couplings are contained in Table 1 where all particle momenta, in squared brackets, are incoming, and $\varphi \equiv (H, \mathcal{H}, A)$.

3.3 Radiatively corrected masses

The mass spectrum satisfies the following tree-level relations:

$$\begin{aligned} m_H &< M_Z |\cos 2\beta| \\ m_H &< m_A \\ m_{H^\pm} &> M_W \end{aligned} \quad (57)$$

which could have a number of very important phenomenological implications, as it is rather obvious. However, it was discovered^{25–28} that radiative corrections are important and can spoil the above tree level relations with a great phenomenological relevance. A detailed knowledge of radiatively corrected couplings and masses is necessary for experimental searches in the MSSM.

The **effective potential** methods to compute the (radiatively corrected) Higgs mass spectrum in the MSSM are useful since they allow to **resum** (using Renormalization Group (RG) techniques) LL, NTLL,..., corrections to **all orders** in perturbation theory. These methods^{25,26}, were first developed in the early nineties.

Vertex	Couplings
$(H, \mathcal{H})WW$	$(\phi WW)_{\text{SM}}[\sin(\beta - \alpha), \cos(\beta - \alpha)]$
$(H, \mathcal{H})ZZ$	$(\phi ZZ)_{\text{SM}}[\sin(\beta - \alpha), \cos(\beta - \alpha)]$
$\varphi[p]W^{\pm}H^{\mp}[k]$	$\mp i\frac{g}{2}(p+k)^{\mu}[\cos(\beta - \alpha), -\sin(\beta - \alpha), \pm i]$
$\varphi u\bar{u}$	$(\phi u\bar{u})_{\text{SM}}[\frac{\cos \alpha}{\sin \beta}, \frac{\sin \alpha}{\sin \beta}, -i\gamma_5 \cot \beta]$
$\varphi d\bar{d}$	$(\phi d\bar{d})_{\text{SM}}[-\frac{\sin \alpha}{\cos \beta}, \frac{\cos \alpha}{\cos \beta}, -i\gamma_5 \tan \beta]$
$H^- u\bar{d}$	$\frac{ig[(m_d \tan \beta + m_u \cot \beta) - (m_d \tan \beta - m_u \cot \beta)\gamma_5]}{2\sqrt{2}M_W}$
$H^+ u\bar{d}$	$\frac{ig[(m_d \tan \beta + m_u \cot \beta) + (m_d \tan \beta - m_u \cot \beta)\gamma_5]}{2\sqrt{2}M_W}$
$(\gamma, Z)H^+[p]H^-[k]$	$-i(p+k)^{\mu} \left[e, g \frac{\cos 2\theta_W}{2 \cos \theta_W} \right]$
$h[p]A[k]Z$	$-\frac{e}{2 \cos \theta_W \sin \theta_W}(p+k)^{\mu} \cos(\beta - \alpha)$

Table 1

Effective potential methods are based on the **run-and-match** procedure by which all dimensionful and dimensionless couplings are running with the RGE scale, for scales greater than the masses involved in the theory. When the RGE scale equals a particular mass threshold, heavy fields decouple, eventually leaving threshold effects in order to match the effective theory below and above the mass threshold. For instance, assuming a common soft supersymmetry breaking mass for left-handed and right-handed stops and sbottoms, $M_S \sim m_Q \sim m_U \sim m_D$, and assuming for the top-quark mass, m_t , and for the CP-odd Higgs mass, m_A , the range $m_t \leq m_A \leq M_S$, we have: for scales $Q \geq M_S$, the MSSM, for $m_A \leq Q \leq M_S$ the two-Higgs doublet model (2HDM), and for $m_t \leq Q \leq m_A$ the SM. Of course there are thresholds effects at $Q = M_S$ to match the MSSM with the 2HDM, and at $Q = m_A$ to match the 2HDM with

the SM.

The case $m_A \sim M_S$

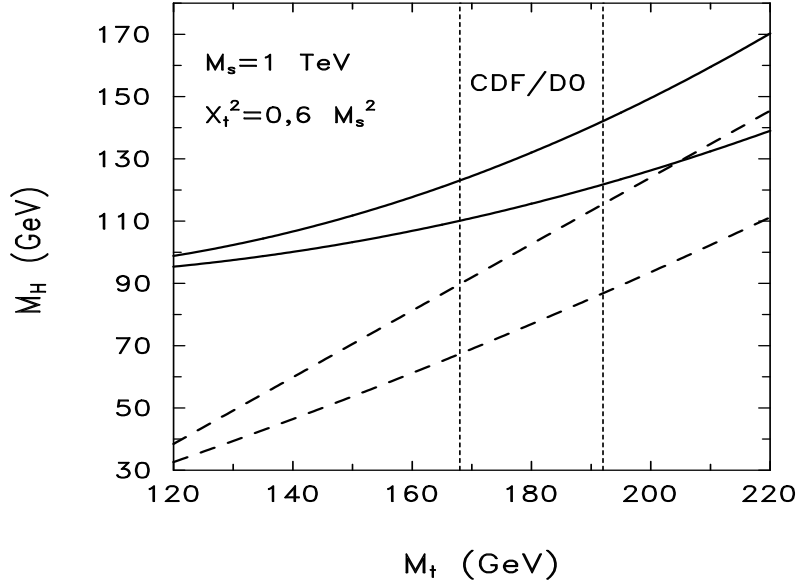


Figure 4: Plot of M_H as a function of M_t for $\tan \beta \gg 1$ (solid lines), $\tan \beta = 1$ (dashed lines), and $X_t^2 = 6M_S^2$ (upper set), $X_t = 0$ (lower set).

The case $m_A \sim M_S$ is, not only a great simplification since the effective theory below M_S is the SM, but also of great interest, since it provides the upper bound on the mass of the lightest Higgs (which is interesting for phenomenological purposes, e.g. at LEP2). In this case we have found^{29,30} that, in the absence of mixing (the case $X_t = 0$) two-loop corrections resum in the one-loop result shifting the energy scale from M_S (the tree-level scale) to $\sqrt{M_S m_t}$. More explicitly,

$$m_H^2 = M_Z^2 \cos^2 2\beta \left(1 - \frac{3}{8\pi^2} h_t^2 t \right) + \frac{3}{2\pi^2 v^2} m_t^4 (\sqrt{M_S m_t}) t \quad (58)$$

where $t = \log(M_S^2/M_t^2)$ and bottom Yukawa coupling is neglected.

In the presence of mixing ($X_t \neq 0$), the run-and-match procedure yields an extra piece in the SM effective potential $\Delta V_{\text{th}}[\phi(M_S)]$ whose second derivative

gives an extra contribution to the Higgs mass, as

$$\Delta_{\text{th}} m_H^2 = \frac{\partial^2}{\partial \phi^2(t)} \Delta V_{\text{th}}[\phi(M_S)] = \frac{1}{\xi^2(t)} \frac{\partial^2}{\partial \phi^2(t)} \Delta V_{\text{th}}[\phi(M_S)] \quad (59)$$

which, in our case, reduces to

$$\Delta_{\text{th}} m_H^2 = \frac{3}{4\pi^2} \frac{m_t^4(M_S)}{v^2(m_t)} \frac{X_t^2}{M_S^2} \left(2 - \frac{1}{6} \frac{X_t^2}{M_S^2} \right) \quad (60)$$

where $X_t = (A_t - \mu/\tan\beta)$ is the mixing in the stop mass matrix, the parameters A_t and μ being the trilinear soft-breaking coupling in the stop sector and the supersymmetric Higgs mixing mass, respectively. The maximum of (60) corresponds to $X_t^2 = 6M_S^2$ which provides the maximum value of the lightest Higgs mass: this case will be referred to as the case of maximal mixing.

We have plotted in Fig. 4 the lightest Higgs pole mass M_H , where all NTLL corrections are resummed to all-loop by the RGE, as a function of M_t ¹⁰. From Fig. 4 we can see that the present experimental band from CDF/D0 for the top-quark mass requires $M_H \lesssim 135$ GeV, while if we fix $M_t = 175$ GeV, the upper bound $M_H \lesssim 125$ GeV follows. It goes without saying that these figures are extremely relevant for MSSM Higgs searches at LEP2.

The case $m_A \lesssim M_S$

The case $m_A \lesssim M_S$ is more complicated since the effective theory below the supersymmetric scale M_S is the 2HDM with λ_i couplings in (40). However since radiative corrections in the 2HDM are equally dominated by the top-quark, we can compute analytical expressions based upon the two loop LL approximation at the scale $Q^2 \sim M_t^2$. Our approximation²⁰ differs from the LL all-loop numerical resummation by $\lesssim 3$ GeV, which we consider the uncertainty inherent in the theoretical calculation, provided the mixing is moderate and, in particular, bounded by the condition,

$$\left| \frac{m_{\tilde{t}_1}^2 - m_{\tilde{t}_2}^2}{m_{\tilde{t}_1}^2 + m_{\tilde{t}_2}^2} \right| \lesssim 0.5 \quad (61)$$

where $\tilde{t}_{1,2}$ are the two stop mass eigenstates.

The above quartic couplings are given by ^f

^fFor simplicity, we neglect the leading D -term contributions and bottom Yukawa coupling effects. The latter may become large for values of $\tan\beta \simeq m_t/m_b$, where m_b is the running bottom mass at the scale M_t . Complete formulae have been worked out²⁹.

$$\Delta\lambda_1 = -\frac{3}{96\pi^2} h_t^4 \frac{\mu^4}{M_S^4} \left[1 + \frac{1}{16\pi^2} (9 h_t^2 - 16g_s^2) t \right] \quad (62)$$

$$\Delta\lambda_2 = \frac{3}{8\pi^2} h_t^4 \left[t + \frac{X_t^0}{2} + \frac{1}{16\pi^2} \left(\frac{3 h_t^2}{2} - 8 g_s^2 \right) (X_t^0 t + t^2) \right] \quad (63)$$

$$\Delta\lambda_3 = \frac{3}{96\pi^2} h_t^4 \left[\frac{3\mu^2}{M_S^2} - \frac{\mu^2 A_t^2}{M_S^4} \right] \left[1 + \frac{1}{16\pi^2} (6 h_t^2 - 16g_s^2) t \right] \quad (64)$$

$$\Delta\lambda_4 = \frac{3}{96\pi^2} h_t^4 \left[\frac{3\mu^2}{M_S^2} - \frac{\mu^2 A_t^2}{M_S^4} \right] \left[1 + \frac{1}{16\pi^2} (6 h_t^2 - 16g_s^2) t \right] \quad (65)$$

$$\Delta\lambda_5 = -\frac{3}{96\pi^2} h_t^4 \frac{\mu^2 A_t^2}{M_S^4} \left[1 + \frac{1}{16\pi^2} (6 h_t^2 - 16g_s^2) t \right] \quad (66)$$

$$\Delta\lambda_6 = \frac{3}{96\pi^2} h_t^4 \frac{\mu^3 A_t}{M_S^4} \left[1 + \frac{1}{16\pi^2} \left(\frac{15}{2} h_t^2 - 16g_s^2 \right) t \right] \quad (67)$$

$$\Delta\lambda_7 = \frac{3}{96\pi^2} h_t^4 \frac{\mu}{M_S} \left(\frac{A_t^3}{M_S^3} - \frac{6A_t}{M_S} \right) \left[1 + \frac{1}{16\pi^2} \left(\frac{9}{2} h_t^2 - 16g_s^2 \right) t \right], \quad (68)$$

where we have defined,

$$X_t^0 = \frac{2A_t^2}{M_S^2} \left(1 - \frac{A_t^2}{12M_S^2} \right). \quad (69)$$

All quantities in the approximate formulae are defined at the scale M_t . For $m_A \leq M_t$, $\tan\beta$ is fixed at the scale m_A , while for $m_A \geq M_t$, $\tan\beta$ is given by²⁸

$$\tan\beta(M_t) = \tan\beta(m_A) \left[1 + \frac{3}{32\pi^2} h_t^2 \log \frac{m_A^2}{M_t^2} \right]. \quad (70)$$

For the case in which the CP-odd Higgs mass m_A is lower than M_S , but still larger than the top-quark mass scale, we decouple, in the numerical computations, the heavy Higgs doublet and define an effective quartic coupling for the light Higgs, which is related to the running Higgs mass at the scale m_A through

$$\lambda(m_A) = \frac{m_h(m_A)}{2v^2}. \quad (71)$$

The low energy value of the quartic coupling is then obtained by running the SM renormalization-group equations from the scale m_A down to the scale M_t . We have defined up to here the running masses. To obtain physical masses we have to use (18) with $\Delta\Pi$ defined in appendix B.

Notice that the knowledge of the radiatively corrected quartic couplings λ_i , $i = 1, \dots, 7$, and hence of the corresponding value of the Higgs mixing angle α , permits the evaluation of all radiatively corrected Higgs couplings in Table 1. In Fig. 5 the Higgs mass spectrum is plotted versus m_A .

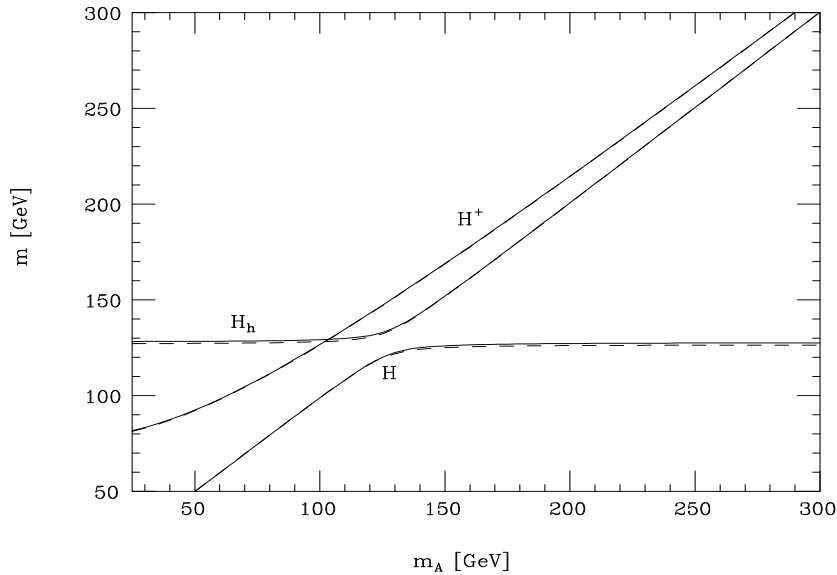


Figure 5: The neutral (H , $\mathcal{H} \equiv H_h$ in the figure) and charged (H^+) Higgs mass spectrum as a function of the CP-odd Higgs mass m_A for a physical top-quark mass $M_t = 175$ GeV and $M_S = 1$ TeV, as obtained from the one-loop improved RGE evolution (solid lines) and the analytical formulae (dashed lines). All sets of curves correspond to $\tan \beta = 15$ and large squark mixing, $X_t^2 = 6M_S^2$ ($\mu = 0$).

There are two possible caveats in the approximation we have just presented: **i)** Our expansion parameter $\log(M_S^2/m_t^2)$ does not behave properly in the supersymmetric limit $M_S \rightarrow 0$, where we should recover the tree-level result. **ii)** We have expanded the threshold function $\Delta V_{\text{th}}[\phi(M_S)]$ to order X_t^4 . In fact keeping the whole threshold function $\Delta V_{\text{th}}[\phi(M_S)]$ we would be able to go to larger values of X_t and to evaluate the accuracy of the approximation (60). Only then we will be able to check the reliability of the maximum

value of the lightest Higgs mass (which corresponds to the maximal mixing) as provided in the previous sections.

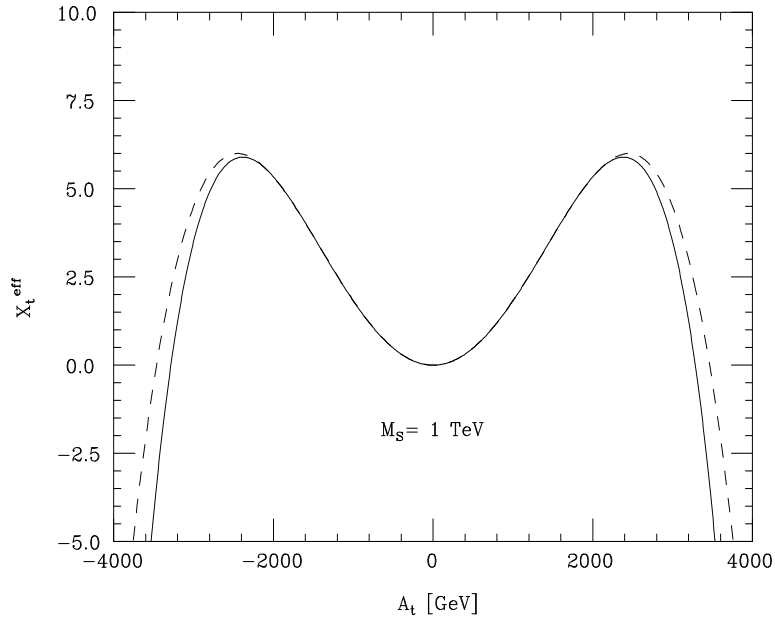


Figure 6: Plot of the exact (solid line) and approximated (dashed line) effective mixing X_t^{eff} as a function of A_t , for $M_S = 1$ TeV and $\mu = 0$.

This procedure has been properly followed in Refs.²⁹ and³¹, where the most general case $m_Q \neq m_U \neq m_D$ has been considered. We have proved that keeping the exact threshold function $\Delta V_{\text{th}}[\phi(M_S)]$, and properly running its value from the high scale to m_t with the corresponding anomalous dimensions as in (59), produces two effects: **i**) It makes a resummation from M_S^2 to $M_S^2 + m_t^2$ and generates as (physical) expansion parameter $\log[(M_S^2 + m_t^2)/m_t^2]$. **ii)** It generates a whole threshold function X_t^{eff} such that (60) becomes

$$\Delta_{\text{th}} m_H^2 = \frac{3}{4\pi^2} \frac{m_t^4 [M_S^2 + m_t^2]}{v^2(m_t)} X_t^{\text{eff}} \quad (72)$$

and

$$X_t^{\text{eff}} = \frac{X_t^2}{M_S^2 + m_t^2} \left(2 - \frac{1}{6} \frac{X_t^2}{M_S^2 + m_t^2} \right) + \dots \quad (73)$$

In fact we have plotted X_t^{eff} as a function of A_t (solid line) and compared with the approximation where we keep only terms up to X_t^4 (dashed line), as we did in the previous sections. The result shows that the maximum of both curves are very close to each other, what justifies the reliability of previous upper bounds on the lightest Higgs mass as, e.g., in Fig. 6

4 Non-minimal Supersymmetric Standard Models

The tree-level bound (57) does no longer hold in supersymmetric models with extra Higgs fields, the so-called NMSSM. We will study in this section Higgs bounds in a general class of NMSSM.

The first (obvious) enlargement of the Higgs sector consists in adding pairs of Higgs doublets $H_1^{(j)}, H_2^{(j)}, j = 1, \dots, N$. These models have been analyzed³² and their lightest scalar Higgs boson shown to have the tree-level bound (57).

Consider now NMSSM with Higgs doublets H_1, H_2 and neutral scalar fields $N_{12}^{(i)}, N_{11}^{(j)}, N_{22}^{(j)}$ (either $SU(2)_L \times U(1)_Y$ singlets or making part of higher dimensional representations) with a cubic superpotential $f = g + f_{YUK}$

$$g = \vec{\lambda} \cdot \vec{N}_{12} H_1^o H_2^o + \sum_{i=1}^2 \vec{\chi}_i \cdot \vec{N}_{ii} (H_i^o)^2, \quad (74)$$

where $\vec{\lambda} \cdot \vec{N} \equiv \sum_j \lambda_j N^{(j)}$ and f_{YUK} contains all Yukawa couplings giving mass to fermions. Then, the lightest scalar Higgs boson mass has an upper bound given by^{33,37}

$$\frac{m_h^2}{v^2} \leq \frac{1}{2} (g^2 + g'^2) \cos^2 2\beta + \vec{\lambda}^2 \sin^2 2\beta + \vec{\chi}_1^2 \cos^4 \beta + \vec{\chi}_2^2 \sin^4 \beta. \quad (75)$$

The bound for the MSSM is recovered from (75) when $\vec{\lambda} = \vec{\chi}_1 = \vec{\chi}_2 = 0$. However in NMSSM some of the Yukawa couplings in (74) can be non-zero. In that case the upper bound on the lightest scalar Higgs boson mass comes from the requirement that the supersymmetric theory remains perturbative up to some scale Λ , in the energy range where the theory holds.

We will keep in f_{YUK} the top and bottom quark Yukawa couplings, *i.e.*

$$f_{YUK} = h_t Q \cdot H_2 U^c + h_b Q \cdot H_1 D^c, \quad (76)$$

with boundary conditions

$$h_t = \frac{g}{\sqrt{2}} \frac{m_t}{m_W} (1 + \cot^2 \beta)^{1/2}, \quad h_b = \frac{g}{\sqrt{2}} \frac{m_b}{m_W} (1 + \tan^2 \beta)^{1/2}. \quad (77)$$

m_t in (77) will be considered as a variable while h_b is fixed by m_b , which is taken to be $m_b(2 m_b) = 5 \text{ GeV}$. For $\tan \beta \gg 1$, h_b can become important. In particular it is comparable to h_t for $\tan \beta \sim m_t/m_b$. h_τ will be neglected since it is given by $h_b(m_\tau/m_b)$ for all values of $\tan \beta$. The cubic g -superpotential in (74) and so the tree-level mass in (75) are model dependent. The latter depends on the couplings $\vec{\lambda}$, $\vec{\chi}_i$ allowed by the perturbative requirement.

4.1 NMSSM with an arbitrary number of singlets

These models are particularly interesting in the sense that the prediction of perturbative unification of the MSSM from LEP precision measurements is not spoiled by the extra matter. They are defined by a Higgs sector containing H_1 , H_2 and n singlets S_i ($i = 1, \dots, n$) with a cubic superpotential

$$g = \vec{\lambda} \cdot \vec{S} H_1 \cdot H_2 + \frac{1}{6} \sum_{i,j,k} \chi_{ijk} S_i S_j S_k. \quad (78)$$

The model with $n = 1$ has been studied in great detail in the literature^{32–40}. The tree-level upper bound on the mass of the lightest scalar Higgs boson for the case of arbitrary n can be written as^{33,36}:

$$m_h^2 \leq (\cos^2 2\beta + \frac{2\vec{\lambda}^2 \cos^2 \theta_W}{g^2} \sin^2 2\beta) m_Z^2. \quad (79)$$

The relevant one-loop RGE are

$$\begin{aligned} 4\pi^2 \dot{\vec{\lambda}}^2 &= \left\{ -\frac{3}{2}g^2 - \frac{1}{2}g'^2 + 2\vec{\lambda}^2 + \frac{3}{2}(h_t^2 + h_b^2) \right\} \vec{\lambda}^2 + \frac{1}{4}\lambda_i \lambda_j \text{tr}(M_i M_j), \\ 8\pi^2 \dot{M}_k &= 3\lambda_k \vec{M} \cdot \vec{\lambda} + \frac{3}{4} \text{tr}(\vec{M} \cdot M_k) \cdot \vec{M}, \\ 8\pi^2 \dot{h}_t &= \left\{ -\frac{3}{2}g^2 - \frac{13}{18}g'^2 - \frac{8}{3}g_s^2 + \frac{1}{2}\vec{\lambda}^2 + 3h_t^2 + \frac{1}{2}h_b^2 \right\} h_t, \\ 8\pi^2 \dot{h}_b &= \left\{ -\frac{3}{2}g^2 - \frac{7}{18}g'^2 - \frac{8}{3}g_s^2 + \frac{1}{2}\vec{\lambda}^2 + \frac{1}{2}h_t^2 + 3h_b^2 \right\} h_b, \end{aligned} \quad (80)$$

Assuming that the theory remains perturbative up to the scale $\Lambda \sim 2 \times 10^{16} \text{ GeV}$, integrating numerically the RGE and including radiative corrections ⁹ for $M_S = 1 \text{ TeV}$ we find ³⁶ the upper bound shown in Fig. 7 in the (m_h, m_t) -plane.

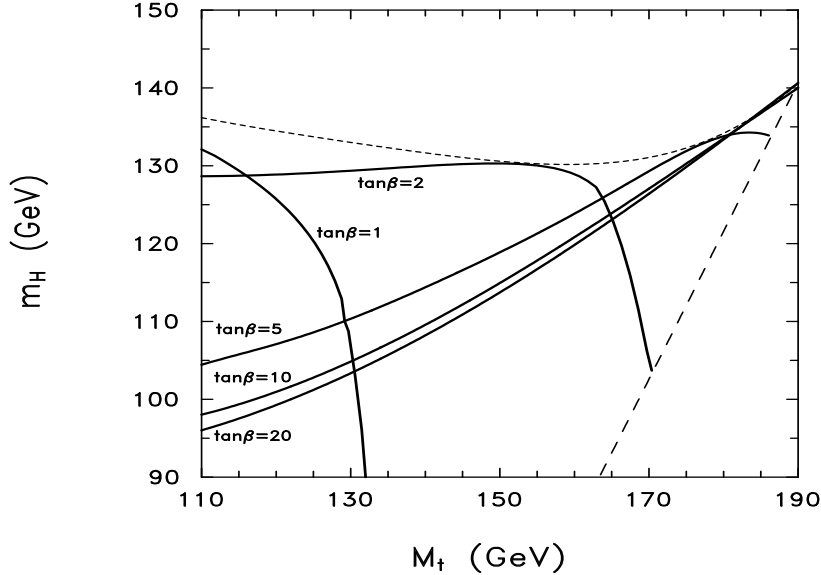


Figure 7: Upper bounds on the lightest scalar Higgs boson in NMSSM with singlets, different values of $\tan \beta$ and maximal mixing in the stop sector.

We see from Fig. 7 that the detailed functional dependence of m_H on M_t is parametrized by the value of $\tan \beta$. The dashed curve where the solid lines stop correspond to values of m_t such that the Yukawa coupling h_t becomes non-perturbative. (For $\tan \beta > 30$ the corresponding lines would follow very close to the $\tan \beta = 20$ curve in Fig. 7, but stopping at lower values of m_t because of the large values of h_b .) The dotted curve on the top of the figure is the enveloping for all values of $\tan \beta$ and can therefore be considered as the absolute upper bound. We obtain from Fig. 7, $m_h \lesssim 140 \text{ GeV}$.

⁹Radiative corrections corresponding to MSSM particles will be retained as in the previous section. We will assume that those corresponding to non-MSSM couplings are negligible. For values of the top-quark mass inside the experimental range the non-MSSM radiative corrections are found to be small, $\lesssim 10 \text{ GeV}$. For a detailed discussion on radiative corrections in these models, see Refs. ^{38,39,40}.

5 What if a Higgs boson is discovered at FNAL or LEP?

If the Higgs turns out to be light, it might be discovered at LEP (for $M_H \lesssim 95$ GeV²²), or even at FNAL (for $M_H \lesssim 120$ GeV, if Tevatron can run until accumulating an integrated luminosity $\int \mathcal{L} \sim 25\text{-}30 \text{ fb}^{-1}$, TeV33 option⁴¹) which could cover all the parameter space of the MSSM and most of the NMSSM one. In this case, the Higgs mass measurement could clearly discriminate between the supersymmetric and non-supersymmetric standard models and, more generally, provide information about the scale of new physics. These two topics will be covered in this section.

5.1 A light Higgs can measure the scale of New Physics

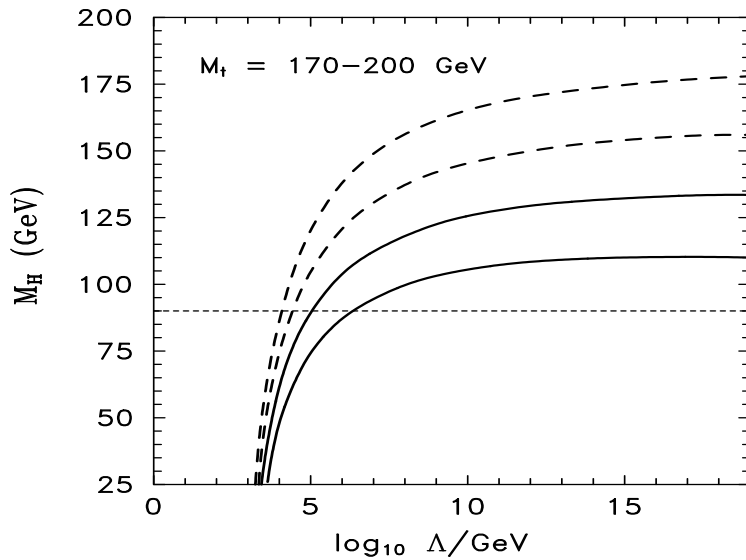


Figure 8: SM lower bounds on M_H from metastability requirements as a function of Λ for different values of M_t .

From the bounds on $M_H(\Lambda)$ previously obtained (see Fig. 8) one can easily deduce that a measurement of M_H will provide an **upper bound** (below the Planck scale) on the scale of new physics provided that

$$M_t[\text{GeV}] > \frac{M_H[\text{GeV}]}{2.25} + 123 \text{ GeV} \quad (81)$$

Thus, the present experimental bound from LEP, $M_H > 67$ GeV, would imply, from (81), $M_t > 153$ GeV, which is fulfilled by experimental detection of the top. Even non-observation of the Higgs at LEP2 (i.e. $M_H \gtrsim 95$ GeV), would leave an open window ($M_t \gtrsim 165$ GeV) to the possibility that a future Higgs detection at FNAL or LHC could lead to an upper bound on Λ . Moreover, Higgs detection at LEP2 would put an upper bound on the scale of new physics. Taking, for instance, $M_H \lesssim 95$ GeV and 170 GeV $< M_t < 180$ GeV, then $\Lambda \lesssim 10^7$ GeV, while for 180 GeV $< M_t < 190$ GeV, $\Lambda \lesssim 10^4$ GeV, as can be deduced from Fig. 8. Finally, using as upper bound for the top-quark mass $M_t < 181$ GeV we obtain from (81) that only if the condition

$$M_h > 128 \text{ GeV} \quad (82)$$

is fulfilled, the SM can be a consistent theory up to the Planck scale, where gravitational effects can no longer be neglected.

5.2 Disentangling between supersymmetric and non-supersymmetric models

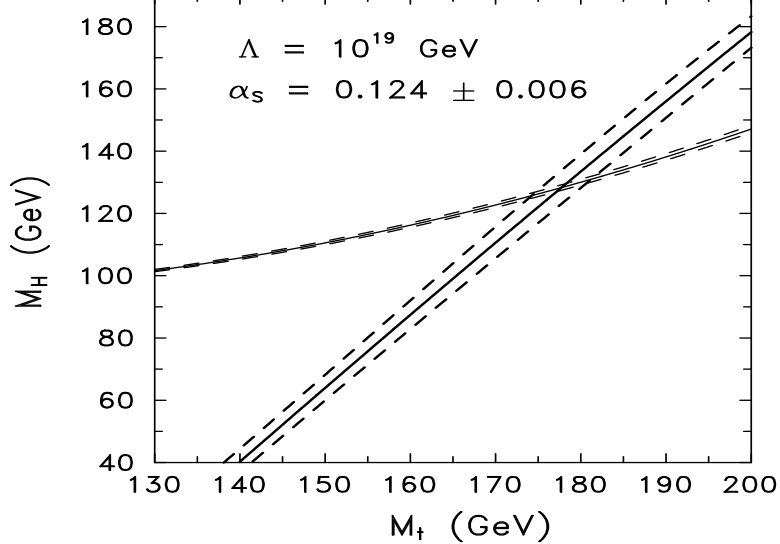


Figure 9: SM lower bounds on M_H (thick lines) as a function of M_t , for $\Lambda = 10^{19}$ GeV, from metastability requirements, and upper bound on the lightest Higgs boson mass in the MSSM (thin lines) for $M_S = 1$ TeV.

We will conclude with a very interesting case, where the Higgs sector of the MSSM plays a key role in the detection of supersymmetry. It is the case where all supersymmetric particles are superheavy, $M_S \sim 1 - 10$ TeV, and escape detection at LHC. In the Higgs sector \mathcal{H}, A, H^\pm decouple, while the H couplings go to the SM ϕ couplings, $HXY \rightarrow (\phi XY)_{\text{SM}}$ as $\sin(\beta - \alpha) \rightarrow 1$, or are indistinguishable from the SM ones [see Table 1], $h_u \sin \beta \equiv h_u^{\text{SM}}$, $h_{d,\ell} \cos \beta \equiv h_{d,\ell}^{\text{SM}}$. In this way the $\tan \beta$ dependence of the couplings, either disappears or is absorbed in the SM couplings.

However, from the previous sections it should be clear that the Higgs and top mass measurements could serve to discriminate between the SM and its extensions, and to provide information about the scale of new physics Λ . In Fig. 9 we give the SM lower bounds on M_H for $\Lambda \gtrsim 10^{15}$ GeV (thick lines) and the upper bound on the mass of the lightest Higgs boson in the MSSM (thin lines) for $M_S \sim 1$ TeV. Taking $M_t = 175$ GeV and $M_H \gtrsim 130$ GeV, the SM is allowed and the MSSM is excluded. On the other hand, if $M_H \lesssim 130$ GeV, then the MSSM is allowed while the SM is excluded. Likewise there are regions where the SM is excluded, others where the MSSM is excluded and others where both are permitted or both are excluded.

6 Conclusion

To conclude, we can say that the search of the Higgs boson at present and future colliders is, not only an experimental challenge, being the Higgs boson the last missing ingredient of the Standard Model, but also a theoretically appealing question from the more fundamental point of view of physics beyond the Standard Model. In fact, if we are lucky enough and the Higgs boson is detected soon (preferably at LEP2) and *light*, its detection might give sensible information about the possible existence of new physics. In that case, the experimental search of the new physics should be urgent and compelling, since the existence of new phenomena might be necessary for our present understanding of physics for energies at reach in the planned accelerators.

Acknowledgements

Work supported in part by the European Union (contract CHRX-CT92-0004) and CICYT of Spain (contract AEN95-0195). I wish to thank my collaborators A. Brignole, M. Carena, J.A. Casas, J.R. Espinosa, H. Haber, G. Kane, J. Moreno, A. Riotto, C. Wagner and F. Zwirner for what I learnt from them.

Appendix A: $\Delta\Pi$ in the SM

The quantity $\Delta\Pi$ in the Landau gauge is given by the sum of the following terms

$$\begin{aligned}
\Delta\Pi &= \Delta\Pi_{tt} \quad (\text{top contribution}) \\
&+ \Delta\Pi_{W^\pm W^\mp} + \Delta\Pi_{Z^0 Z^0} \\
&+ \Delta\Pi_{W^\pm \chi^\mp} + \Delta\Pi_{Z^0 \chi_3} \quad (\text{gauge and Goldstone bosons contribution}) \\
&+ \Delta\Pi_{\chi^\pm \chi^\mp} + \Delta\Pi_{\chi_3 \chi_3} \\
&+ \Delta\Pi_{HH} \quad (\text{pure scalar bosons contribution}). \tag{A.1}
\end{aligned}$$

In Eq. (A.1) we have taken into account only the contribution from the heaviest fermion, the top, and indicated by χ^\pm and χ_3 the charged and the neutral Goldstone bosons, respectively.

The complete expression¹⁰ for the different contributions to (real part of) $\Delta\Pi$ calculated in the \overline{MS} scheme is, for $M_H < 2M_W$:

$$\Delta\Pi_{tt} = \frac{3h_t^2}{8\pi^2} \left\{ -2M_t^2 \left[Z\left(\frac{M_t^2}{M_H^2}\right) - 2 \right] + \frac{1}{2}M_H^2 \left[\log \frac{M_t^2}{\mu^2} + Z\left(\frac{M_t^2}{M_H^2}\right) - 2 \right] \right\}. \tag{A.2}$$

where $Z(x)$ is the function

$$\begin{aligned}
Z(x) &= \begin{cases} 2A \tan^{-1}(1/A), & \text{if } x > 1/4 \\ A \log [(1+A)/(1-A)], & \text{if } x < 1/4 \end{cases} \\
A &\equiv |1 - 4x|^{1/2}. \tag{A.3}
\end{aligned}$$

$$\begin{aligned}
&\Delta\Pi_{W^\pm W^\mp} + \Delta\Pi_{Z^0 Z^0} + \Delta\Pi_{W^\pm \chi^\mp} + \Delta\Pi_{Z^0 \chi_3} \\
&= \frac{g^2 M_W^2}{8\pi^2} \left[-3 + \frac{5}{4} \frac{M_H^2}{M_W^2} + \frac{1}{2} \left(3 - \frac{M_H^2}{M_W^2} + \frac{M_H^4}{4M_W^4} \right) Z\left(\frac{M_W^2}{M_H^2}\right) - \frac{M_H^4}{8M_W^4} \log \frac{M_H^2}{M_W^2} \right. \\
&\quad \left. - \frac{3M_H^2}{4M_W^2} \log \frac{M_W^2}{\mu^2} + \frac{i\pi}{8} \frac{M_H^2}{M_W^2} \right] + \frac{1}{2} \begin{cases} M_W \rightarrow M_Z \\ g^2 \rightarrow g^2 + g'^2 \end{cases}. \tag{A.4}
\end{aligned}$$

The contribution to $\Delta\Pi$ coming from the pure scalar sector deserves more attention. In the Landau gauge the Goldstone bosons χ 's do have a field dependent mass $m_\chi(\phi) = -m^2 + \lambda\phi^2/2$ which vanishes at the minimum of the potential $V_{\text{eff}}(\phi)$. As a consequence, the running mass m_H presents an infrared logarithmic divergence when Goldstone bosons are included in the

effective potential V_{eff} , which is cancelled by an equal (and opposite in sign) contribution of the same excitations to $\Delta\Pi$. Explicitly,

$$\Delta M_H^2 = \frac{3}{128\pi^2} \frac{g^2 M_H^4}{M_W^2} \left[\pi\sqrt{3} - 8 + 4 \log \frac{M_H^2}{m_t^2} \right]. \quad (\text{A.5})$$

Appendix B: $\Delta\Pi$ in the MSSM

We first define the different self-energy contributions as

$$\Delta\Pi_\varphi(M_\varphi^2) = \Delta\Pi_\varphi^{(t)}(M_\varphi^2) + \Delta\Pi_\varphi^{(b)}(M_\varphi^2) + \Delta\Pi_\varphi^{(\tilde{t})}(M_\varphi^2) + \Delta\Pi_\varphi^{(\tilde{b})}(M_\varphi^2) \quad (\text{B.1})$$

where $\varphi = H, \mathcal{H}, A$. The different contributions in (B.1) read:

$$\Delta\Pi_H^{(t)}(M_H^2) = \frac{3}{8\pi^2} h_t^2 \cos^2 \alpha \left[-2M_t^2 + \frac{1}{2}M_H^2 \right] f(M_t^2, M_t^2, M_H^2) \quad (\text{B.2})$$

$$\Delta\Pi_{\mathcal{H}}^{(t)}(M_{\mathcal{H}}^2) = \frac{3}{8\pi^2} h_t^2 \sin^2 \alpha \left[-2M_t^2 + \frac{1}{2}M_{\mathcal{H}}^2 \right] f(M_t^2, M_t^2, M_{\mathcal{H}}^2) \quad (\text{B.3})$$

$$\Delta\Pi_A^{(t)}(M_A^2) = \frac{3}{8\pi^2} h_t^2 \cos^2 \beta \left[-\frac{1}{2}M_A^2 \right] f(M_t^2, M_t^2, M_A^2) \quad (\text{B.4})$$

$$\Delta\Pi_H^{(b)}(M_H^2) = \frac{3}{8\pi^2} h_b^2 \sin^2 \alpha \left[-2m_b^2 + \frac{1}{2}M_H^2 \right] f(m_b^2, m_b^2, M_H^2) \quad (\text{B.5})$$

$$\Delta\Pi_{\mathcal{H}}^{(b)}(M_{\mathcal{H}}^2) = \frac{3}{8\pi^2} h_b^2 \cos^2 \alpha \left[-2m_b^2 + \frac{1}{2}M_{\mathcal{H}}^2 \right] f(m_b^2, m_b^2, M_{\mathcal{H}}^2) \quad (\text{B.6})$$

$$\Delta\Pi_A^{(b)}(M_A^2) = \frac{3}{8\pi^2} h_b^2 \sin^2 \beta \left[-\frac{1}{2}M_A^2 \right] f(m_b^2, m_b^2, M_A^2) \quad (\text{B.7})$$

$$\Delta\Pi_\varphi^{(\tilde{t})}(M_\varphi^2) = \sum_{i,j=1}^2 \frac{3}{16\pi^2} \left| C_{\varphi ij}^{(\tilde{t})} \right|^2 f(m_{\tilde{t}_i}^2, m_{\tilde{t}_j}^2, M_\varphi^2) \quad (\text{B.8})$$

$$\Delta\Pi_\varphi^{(\tilde{b})}(M_\varphi^2) = \sum_{i,j=1}^2 \frac{3}{16\pi^2} \left| C_{\varphi ij}^{(\tilde{b})} \right|^2 f(m_{\tilde{b}_i}^2, m_{\tilde{b}_j}^2, M_\varphi^2) \quad (\text{B.9})$$

The different coefficients in (B.8) and (B.9) are:

$$\begin{aligned} C_{Hij}^{(\tilde{t})} &= \frac{2\sqrt{2}\sin^2\theta_W}{3} \frac{M_Z^2}{v} \sin(\beta + \alpha) \left[\delta_{ij} + \frac{3 - 8\sin^2\theta_W}{4\sin^2\theta_W} Z_U^{1i} Z_U^{1j} \right] \\ &- \sqrt{2}h_t^2 v \sin\beta \cos\alpha \delta_{ij} - \frac{1}{\sqrt{2}}h_t(A_t \cos\alpha + \mu \sin\alpha)(Z_U^{1i*} Z_U^{2j} + Z_U^{1j} Z_U^{2i*}) \end{aligned} \quad (\text{B.10})$$

$$\begin{aligned}
C_{\mathcal{H}ij}^{(\tilde{t})} &= -\frac{2\sqrt{2}\sin^2\theta_W}{3}\frac{M_Z^2}{v}\cos(\beta+\alpha)\left[\delta_{ij}+\frac{3-8\sin^2\theta_W}{4\sin^2\theta_W}Z_U^{1i}Z_U^{1j}\right] \quad (\text{B.11}) \\
&- \sqrt{2}h_t^2v\sin\beta\sin\alpha\delta_{ij}-\frac{1}{\sqrt{2}}h_t(A_t\sin\alpha-\mu\cos\alpha)(Z_U^{1i*}Z_U^{2j}+Z_U^{1j}Z_U^{2i*})
\end{aligned}$$

$$C_{Aij}^{(\tilde{t})} = -\frac{1}{\sqrt{2}}h_t(A_t\cos\beta+\mu\sin\beta)(Z_U^{1i*}Z_U^{2j}-Z_U^{1j}Z_U^{2i*}) \quad (\text{B.12})$$

$$\begin{aligned}
C_{Hij}^{(\tilde{b})} &= -\frac{\sqrt{2}\sin^2\theta_W}{3}\frac{M_Z^2}{v}\sin(\beta+\alpha)\left[\delta_{ij}+\frac{3-4\sin^2\theta_W}{2\sin^2\theta_W}Z_D^{1i}Z_D^{1j}\right] \quad (\text{B.13}) \\
&+ \sqrt{2}h_b^2v\cos\beta\sin\alpha\delta_{ij}+\frac{1}{\sqrt{2}}h_b(A_b\sin\alpha+\mu\cos\alpha)(Z_D^{1i*}Z_D^{2j}+Z_D^{1j}Z_D^{2i*})
\end{aligned}$$

$$\begin{aligned}
C_{\mathcal{H}ij}^{(\tilde{b})} &= \frac{\sqrt{2}\sin^2\theta_W}{3}\frac{M_Z^2}{v}\cos(\beta+\alpha)\left[\delta_{ij}+\frac{3-4\sin^2\theta_W}{2\sin^2\theta_W}Z_D^{1i}Z_D^{1j}\right] \quad (\text{B.14}) \\
&- \sqrt{2}h_b^2v\cos\beta\cos\alpha\delta_{ij}-\frac{1}{\sqrt{2}}h_b(A_b\cos\alpha-\mu\sin\alpha)(Z_D^{1i*}Z_D^{2j}+Z_D^{1j}Z_D^{2i*})
\end{aligned}$$

$$C_{Aij}^{(\tilde{b})} = \frac{1}{\sqrt{2}}h_b(A_b\sin\beta+\mu\cos\beta)(Z_D^{1i*}Z_D^{2j}-Z_D^{1j}Z_D^{2i*}), \quad (\text{B.15})$$

where the matrices Z_U^{ij} and Z_D^{ij} are those diagonalizing the stop and sbottom squared mass matrices, respectively, and the function $f(m_1^2, m_2^2, q^2)$ which arises from the integration of the loop of (scalar) particles, is given by

$$f(m_1^2, m_2^2, q^2) = -1 + \frac{1}{2}\left(\frac{m_1^2 + m_2^2}{m_1^2 - m_2^2} - \delta\right)\log\frac{m_2^2}{m_1^2} + \frac{1}{2}r\log\left[\frac{(1+r)^2 - \delta^2}{(1-r)^2 - \delta^2}\right]$$

with $\delta = (m_1^2 - m_2^2)/q^2$ and $r = \sqrt{(1+\delta)^2 - \frac{4m_1^2}{q^2}}$

References

1. S. Coleman and E. Weinberg, *Phys. Rev.* **D7** (1973) 1888.
2. R. Jackiw, *Phys. Rev.* **D9** (1974) 1686.
3. J. Iliopoulos, C. Itzykson and A. Martin, *Rev. Mod. Phys.* **47** (1975) 165.
4. B. Kastening, *Phys. Lett.* **B283** (1992) 287.
5. C. Ford, D.R.T. Jones, P.W. Stephenson and M.B. Einhorn, *Nucl. Phys.* **B395** (1993) 83.

6. M. Bando, T. Kugo, N. Maekawa and H. Nakano, *Phys. Lett.* **B301** (1993) 83; *Prog. Theor. Phys.* **90** (1993) 405.
7. C. Ford, *Phys. Rev.* **D50** (1994) 7531.
8. G. 't Hooft and M. Veltman, *Nucl. Phys.* **B61** (1973) 455; W. A. Bardeen, A.J. Buras, D.W. Duke and T. Muta, *Phys. Rev.* **D18** (1978) 3998.
9. W. Siegel, *Phys. Lett.* **B84** (1979) 193; D.M. Capper, D.R.T. Jones and P. van Nieuwenhuizen, *Nucl. Phys.* **B167** (1980) 479
10. J.A. Casas, J.R. Espinosa, M. Quirós and A. Riotto, *Nucl. Phys.* **B436** (1995) 3; (E) **B439** (1995) 466.
11. N. Cabibbo, L. Maiani, G. Parisi and R. Petronzio, *Nucl. Phys.* **B158** (1979) 295; M. Lindner, *Z. Phys.* **C31** (1986) 295; M. Sher, *Phys. Rep.* **179** (1989) 273; M. Lindner, M. Sher and H.W. Zaglauer, *Phys. Lett.* **B228** (1989) 139; M. Sher, *Phys. Lett.* **B317** (1993) 159; Addendum: *Phys. Lett.* **B331** (1994) 448; C. Ford, D.R.T. Jones, P.W. Stephenson and M.B. Einhorn, *Nucl. Phys.* **B395** (1993) 17.
12. G. Altarelli and I. Isidori, *Phys. Lett.* **B337** (1994) 141.
13. J.A. Casas, J.R. Espinosa and M. Quirós, *Phys. Lett.* **B342** (1995) 171; J.A. Casas, J.R. Espinosa and M. Quirós, *Phys. Lett.* **B382** (1996) 374.
14. J.R. Espinosa and M. Quirós, *Phys. Lett.* **B355** (1995) 257
15. W. Loinaz and R.S. Willey, preprint UP-HEP-9702 [hep-ph/9702321]
16. For a recent review, see, e.g.: M. Quirós, *Helv. Phys. Acta* **67** (1994) 451.
17. L. Dolan and R. Jackiw, *Phys. Rev.* **D9** (1974) 3320; S. Weinberg, *Phys. Rev.* **D9** (1974) 3357; D.J. Gross, R.D. Pisarski and L.G. Yaffe, *Rev. Mod. Phys.* **53** (1981) 43; M.E. Carrington, *Phys. Rev.* **D45** (1992) 2933; M.E. Shaposhnikov, *Phys. Lett.* **B277** (1992) 324 and (E) *Phys. Lett.* **B282** (1992) 483; M. Dine, R.G. Leigh, P. Huet, A. Linde and D. Linde, *Phys. Lett.* **B283** (1992) 319 and *Phys. Rev.* **D46** (1992) 550; J.R. Espinosa and M. Quirós, *Phys. Lett.* **B305** (1993) 98; J.R. Espinosa, M. Quirós and F. Zwirner, *Phys. Lett.* **B314** (1993) 206; C.G. Boyd, D.E. Brahm and S.D. Hsu, *Phys. Rev.* **D48** (1993) 4963; P. Arnold and O. Espinosa, *Phys. Rev.* **D47** (1993) 3546; W. Buchmüller, T. Helbig and D. Walliser, *Nucl. Phys.* **B407** (1993) 387.
18. A.D. Linde, *Phys. Lett.* **B70** (1977) 306; *Phys. Lett.* **B100** (1981) 37; *Nucl. Phys.* **B216** (1983) 421.
19. S. Coleman, *Phys. Rev.* **D15** (1977) 2929.
20. J.I. Kapusta, *Finite temperature field theory* (Cambridge University Press, 1989)
21. P. Arnold and S. Vokos, *Phys. Rev.* **D44** (1991) 3620.
22. Higgs Physics Working Group (convs. M. Carena and P. Zerwas), in

Vol. 1 of *Physics at LEP2*, G. Altarelli, T. Sjostrand and F. Zwirner, eds., Report CERN 96-01, Geneva (1996).

23. H.P. Nilles, *Phys. Rep.* **110** (1984) 1; H.E. Haber and G.L. Kane, *Phys. Rep.* **117** (1985) 75; R. Barbieri, *Riv. Nuovo Cim.* **11** (1988) 1.
24. See, e.g., J.F. Gunion, H.E. Haber, G.L. Kane and S. Dawson, *The Higgs Hunter's Guide*, Addison-Wesley 1990.
25. Y. Okada, M. Yamaguchi and T. Yanagida, *Prog. Theor. Phys.* **85** (1991) 1; *Phys. Lett.* **B262** (1991) 54; J. Ellis, G. Ridolfi and F. Zwirner, *Phys. Lett.* **B257** (1991) 83; *Phys. Lett.* **B262** (1991) 477; R. Barbieri and M. Frigeni, *Phys. Lett.* **B258** (1991) 395; R. Barbieri, M. Frigeni and F. Caravaglios, *Phys. Lett.* **B258** (1991) 167.
26. J.R. Espinosa and M. Quirós, *Phys. Lett.* **B266** (1991) 389.
27. H.E. Haber and R. Hempfling, *Phys. Rev. Lett.* **66** (1991) 1815; A. Yamada, *Phys. Lett.* **B263** (1991) 233.
28. A. Brignole, *Phys. Lett.* **B277** (1992) 313; *Phys. Lett.* **B281** (1992) 284.
29. M. Carena, J.R. Espinosa, M. Quirós and C.E.M. Wagner, *Phys. Lett.* **B355** (1995) 209.
30. H.E. Haber and R. Hempfling, *Phys. Rev.* **D48** (1993) 4280; H.E. Haber, R. Hempfling and A.H. Hoang, preprint CERN-TH/95-216, and TTP95-09 (1995) [hep-ph/9609331].
31. M. Carena, M. Quirós and C.E.M. Wagner, *Nucl. Phys.* **B461** (1996) 407.
32. M. Drees, *Int. J. Mod. Phys.* **A4** (1989) 3635.
33. J.R. Espinosa and M. Quirós, *Phys. Lett.* **B279** (1992) 92.
34. J. Ellis, J. F. Gunion, H. E. Haber, L. Roszkowski and F. Zwirner, *Phys. Rev.* **D39** (1989) 844.
35. P. Binétruy and C. Savoy, *Phys. Lett.* **B277** (1992) 453.
36. J.R. Espinosa and M. Quirós, *Phys. Lett.* **B302** (1993) 51.
37. G.L. Kane, C. Kolda and J. Wells, *Phys. Rev. Lett.* **70** (1993) 2686.
38. U. Ellwanger and M. Rausch de Traubbenger, *Z. Phys.* **C53** (1992) 521; U. Ellwanger and M. Lindner, *Phys. Lett.* **B301** (1993) 365; U. Ellwanger, *Phys. Lett.* **B303** (1993) 271.
39. T. Elliot, S.F. King and P.L. White, *Phys. Lett.* **B305** (1993) 71; *Phys. Lett.* **B314** (1993) 56; *Phys. Rev.* **D49** (1994) 2435; *Phys. Lett.* **B351** (1995) 213.
40. U. Ellwanger, M. Rausch de Traubbenger and C. Savoy, *Phys. Lett.* **B315** (1993) 331; *Z. Phys.* **C67** 665; e-print [hep-ph/9611251].
41. A. Stange, W. Marciano and S. Willenbrock, *Phys. Rev.* **D49** (1994) 1354; *Phys. Rev.* **D50** (1994) 4491.